Faraday instability of superfluid surface

Haruka Abe, Tetsuto Ueda, Michihiro Morikawa, Yu Saitoh, Ryuji Nomura,* and Yuichi Okuda
Department of Condensed Matter Physics, Tokyo Institute of Technology, 2-12-1 O-okayama, Meguro, Tokyo 152-8551, Japan
(Received 23 March 2007; revised manuscript received 13 June 2007; published 5 October 2007)

We observed that Faraday waves are parametrically generated on a free surface of superfluid ^{4}He when a sample cell is vibrated vertically. Standing-wave patterns appear on the surface, and their frequencies are one-half the driving frequency. We observed clear threshold amplitudes of the vibration for the instability. The difference in the threshold between the superfluid and the normal fluid is explained by a wall damping.

DOI: 10.1103/PhysRevE.76.046305 PACS number(s): 47.50.Gj, 47.35.−i, 67.55.Fa, 68.03.Kn

I. INTRODUCTION

Waves are parametrically excited on the free surface of a fluid when its container is vibrated in the vertical direction. This phenomenon is called Faraday instability [1]. The vertical vibration of the container is equivalent to a periodic modulation of the gravity acceleration and the instability is described by the Mathieu equation. It is regarded as a model system for the physics of pattern formation and nonlinear dynamics [2–10]. To date experiments have been performed only in viscous fluids and no measurement has been made in a superfluid. It is not known how the superfluid ^{4}He reacts to the parametric driving or how the two-fluid hydrodynamics modifies the behavior. We visually observed that Faraday waves were parametrically generated on a free surface of ^{4}He both in the normal fluid at 3.7 K and in the superfluid at very low temperatures, 400 and 700 mK, where the fraction of the normal component is negligible. A Faraday wave was generated at one-half of the driving frequency above the threshold of the vibration amplitude. The threshold amplitude was larger in the normal fluid than in the superfluid.

Other types of instabilities have been found in the interfaces of superfluid He and allowed an understanding of the instability problems in the viscous-free limit. Leiderer observed a period doubling of a charged surface wave of superfluid ^{4}He in a large electric driving field [11]. Kim *et al.* reported that superfluid fog can be generated on the free surface through the Rayleigh-Taylor instability by a strong acoustic driving of the surface [12]. Shear flow between the *A* and *B* phases in superfluid ^{3}He causes the Kelvin-Helmholtz instability [13]. Recently, Faraday waves were found in a Bose-Einstein condensate of ultracold gases [14].

II. EXPERIMENT

We were able to vibrate a sample cell containing liquid ^{4}He vertically while keeping it at a very low temperature. Experiments were performed in an optical dilution refrigerator [15,16], and the superfluid free surface was observed visually. As shown in Fig. 1, the sample cell consisted of a polycarbonate cup, a brass middle flange, and a copper top flange. The polycarbonate cup (*E*) was polished so that it was clear and its interior could be seen. It was 26 mm in inner diameter, 36 mm in outer diameter, and 50 mm in height with a flat bottom. The brim of the cup was threaded so that it fixed to the brass flange and was glued to it by Stycast 1266. The copper flange had sintered silver for a heat exchanger and sealed the brass flange by an In wire. The sample cell was made light enough, about 300 g, so that it was vibrated easily. Two plate springs of stainless steel (*C*) supported the cell. It was thermally anchored to the mixing chamber through annealed copper wires, which were long and gently bent so that they did not prevent the vibration. The lowest temperature achieved was 100 mK in this setup. The depth of the liquid ^{4}He was about 3 mm.

The sample cell had a cylindrical SmCo permanent magnet (*A*) on the top flange, whose diameter and height were 13 mm and 12 mm. The magnet was positioned at the center of an anti-Helmholz superconducting coil (*B*). The coil had an inductance of about 50 mH and a total resistance including a high-temperature region of 21 Ω. We could vibrate the sample cell by applying an ac current to the coil. The resonance frequency of the vertical vibration of the sample cell was 33 Hz, and the half width was 4 Hz. In order to calibrate the amplitude of the vibration, *A*, we applied current to the coil which was a few times larger than that used for the experiment so that the vibration of the cell was large enough to be seen. The vibration was recorded by a high-speed camera at each frequency used for the experiment. We estimated the amplitude in the smaller current assuming a linear response, and the uncertainty of the amplitude was about 10%.

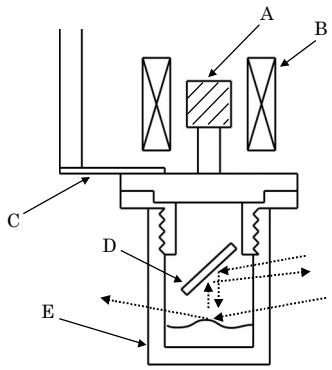

FIG. 1. Schematics of the experimental setup. *A*: SmCo magnet. *B*: anti-Helmholz superconducting coil. *C*: plate spring. *D*: mirror. *E*: polycarbonate cup. Dotted arrows represent the two optical paths used in the experiment (see text).

*nomura@ap.titech.ac.jp

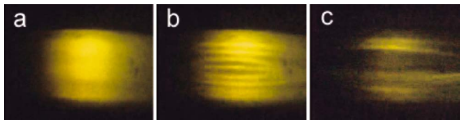

FIG. 2. (Color online) Superfluid free surface of ^{4}He at 700 mK. It was flat when the sample cell was at rest (a). Once the sample cell started to be vibrated at $t=0$ above a threshold amplitude at frequency $f_0=24.0$ Hz, standing waves developed on the surface as (b) at $t=5$ s and (c) at $t=47$ s.

A can be converted to the modulation of the gravity acceleration as $\delta g=A(2\pi f_0)^2$ at a driving frequency of f_0.

Two configurations of the optical setups were used to view the superfluid free surface. The surface was illuminated from a back window in both cases. We recorded the image through a front window using a high-quality camera or the reflected image by a mirror (D) over the surface through the back window using a high-speed camera. The former is suitable for observing a large part of the surface to see its profile and the latter for a part of the surface to obtain information about the wave in a frequency domain. Figure 2 is the profile of the surface by the high-quality camera. The camera looked slightly downward upon the surface at an angle of about 20°. Figure 2(a) is an image of the flat free surface without vibration at $T=700$ mK. We turned on the vibration of the sample cell at $t=0$ s at $f_0=24.0$ Hz and $\delta g=0.27$ m/s^2. Standing waves developed on the surface as in Fig. 2(b) ($t=5$ s) and reached a steady state as in Fig. 2(c) ($t=47$ s). With this vibration, the temperature rose at most several mK.

Brightness I at a particular point in the high-speed camera image was fast Fourier transformed in order to analyze the amplitude of the wave in a frequency domain. Using several points in the image, we checked that results did not depend on which points were used for the analysis. Fourier spectra of I after reaching the steady state are shown in Fig. 3, where $T=700$ mK and $f_0=24.0$ Hz as in Fig. 2. Crosses, triangles, squares, and circles are at $\delta g=0.14$, 0.20, 0.23, and 0.34 m/s^2, respectively. We can clearly see that standing waves were generated at one-half of the vibration frequency and were parametrically excited. This is the necessary condition for the Faraday instability. Large Faraday waves were excited at driving frequencies of $f_0=24.0$, 27.1, 28.3, 29.4, 29.9, 41.0, 42.2, and 43.2 Hz in the superfluid and $f_0=28.6$, 29.8, and 41.1 Hz in the normal fluid. Width of this resonance was typically a few 0.1 Hz.

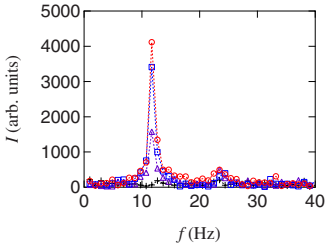

FIG. 3. (Color online) Fourier spectra of brightness I at a particular point of a superfluid surface at $T=700$ mK and $f_0=24.0$ Hz. Crosses, triangles, squares, and circles are at $\delta g=0.14$, 0.20, 0.23, and 0.34 m/s^2, respectively.

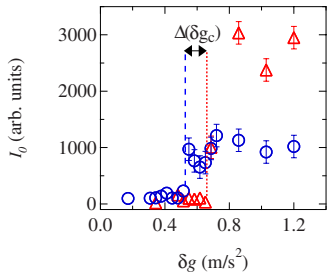

FIG. 4. (Color online) Peak intensities I_0 of the Fourier spectra at the Faraday resonance are plotted as δg at $f_0=29.8$ Hz. Circles are in the superfluid phase at $T=700$ mK, and triangles are in the normal phase at $T=3.7$ K. A clear threshold appears for the instability: $\delta g_c=0.53$ m/s^2 at 700 mK (the dashed line) and $\delta g_c=0.67$ m/s^2 at 3.7 K (the dotted line). The difference is $\Delta(\delta g_c)=0.14$ m/s^2.

III. RESULTS AND DISCUSSION

In Fig. 4, the peak intensities I_0 of the Fourier spectra at the Faraday resonance are plotted as δg. In this case $f_0=29.8$ Hz, where instability occurred in both the superfluid and the normal fluid. Circles are in the superfluid phase at $T=700$ mK, and triangles are in the normal phase at $T=3.7$ K. I_0 stayed near 0 in small δg but became finite in large δg. There exists a threshold value δg_c for the wave excitation in both the superfluid and the normal fluid: $\delta g_c=0.53$ m/s^2 in the superfluid at 700 mK (dashed line) and $\delta g_c=0.67$ m/s^2 in the normal fluid at 3.7 K (dotted line). At 400 mK, δg_c was almost the same as at 700 mK. In the superfluid phase we need smaller excitation for the instability than in the normal fluid phase and the difference in the threshold is $\Delta(\delta g_c)=0.14$ m/s^2. Similar behavior was observed at other frequencies. Although the scatter of data in the instability region is rather large, data in the stable region have much smaller noise, and thus we can easily tell when the system enter the instability region. Error bars in the instability region were determined by a fluctuation of the peak intensity. The fluctuation was larger in the instability region than in the stable region, probably because of a higher sen-

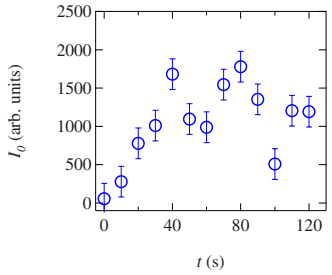

FIG. 5. (Color online) Peak intensities I_0 as a function of time t at $f_0=29.8$ Hz, $\delta g=0.88$ m/s^2, and $T=700$ mK in the superfluid phase.

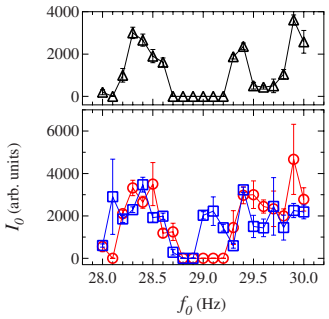

FIG. 6. (Color online) Hysteretic behavior of Faraday waves at $T=700$ mK when a driving frequency was swept. Circles (squares) indicate increasing (decreasing) frequency, and triangles are the case started from rest. A bistable region is clearly seen.

sitivity to the external mechanical noise in the instability region. Note that absolute values of I_0 have no meaning in this figure because the illumination conditions were not always the same at different temperatures. Although I_0 is larger in the normal phase than in the superfluid phase, this does not mean that Faraday waves are larger in the normal phase.

I_0 is plotted as a function of time t in Fig. 5 to see the evolution of the Faraday instability. In this case, $f_0=29.8$ Hz and $\delta g=0.88$ m/s^2 in the superfluid phase at $T=700$ mK. Similar parameters were used for the hysteresis measurement described in the next paragraph. Growth of the peak intensity is clearly seen, and it took about 30 s for the instability to fully develop in this driving force. Even after $t>40$ s, the signal shows a large scatter due to the sensitivity to the external mechanical noise mentioned above.

A clear hysteretic behavior was observed at $T=700$ mK when a driving frequency was swept as Miles theoretically predicted in nonlinear Faraday resonance [6]. The driving frequency was initially set at $f_0=28.0$ Hz, increased to 30.0 Hz, and decreased to 28.0 Hz again. The increment and the decrement were 0.1 Hz and $\delta g\sim 0.88$ m/s^2. At each frequency we waited for 50 s for the system to reach equilibrium and took the spectrum of the wave. The amplitude of the Faraday wave at each frequency was estimated by fitting the resonance in the Fourier spectrum. Circles indicate the increment and squares the decrement in the lower panel of Fig. 6. In order to see the behavior not influenced by its history, we also checked whether or not the wave was generated when started from rest. The system was kept at rest for 60 s before the driving and spectra were measured 50 s after the driving when it reached a steady state. The amplitude of the wave is plotted by triangles in the upper panel of Fig. 6. When started from rest no Faraday wave was generated at f_0 between 28.7 and 29.2 Hz. However, we could retain the wave in this stable range if it was coming from the unstable region as seen in Fig. 6. The wave was still generated at $f_0=28.7$ Hz when coming from the low-frequency unstable region and in the range between 29.0 and 29.2 Hz coming from the high-frequency region.

Surface waves in a cylindrical geometry can be expanded in terms of the orthogonal sets $S_{l,m}(r,\theta)$ using the Bessel function J_l as [2]

$$S_{l,m}(r,\theta)=J_l(k_{l,m}r)\times\begin{cases}\sin l\theta,\\ \cos l\theta,\end{cases} \tag{1}$$

where $k_{l,m}$ is the mth zero of $J_l'(k_{l,m}R)$ assuming a 90° contact angle and $R=13$ mm. The frequency of each mode can be given in a deep-wave approximation as

$$\omega_{l,m}^2=\frac{\alpha k_{l,m}^3}{\rho}+k_{l,m}g, \tag{2}$$

where α, ρ, and g are surface tension, density of liquid, and gravity acceleration, respectively. The observed mode in Fig. 2 looks like a radial mode and is likely to be the $l=0$ and $m=2$ modes, whose frequency is close to the observed frequency 12 Hz. Not all other modes observed are $l=0$, and the eigenfrequencies come close to each other. We have many possibilities for the modes and are unable to successfully identify them.

The Faraday instability problem can be mapped to the Mathieu equation. The amplitude of a mode a in the presence of a vertical vibration is described by the Mathieu equation [2]

$$\frac{d^2a}{dt^2}+\omega_{l,m}^2(1-\epsilon\cos\omega t)a=0, \tag{3}$$

where $\epsilon=k_{l,m}A\omega^2/\omega_{l,m}^2$. Once a parametric resonance condition is met, $\omega=2\omega_{l,m}$, a increases in the $t\to\infty$ limit without any threshold amplitude in the vibration and the mode becomes unstable.

For a viscous fluid, a damping term $\gamma\frac{da}{dt}$ is added to the left hand side of Eq. (3), where γ is proportional to the dissipation in the system. This term stabilizes the flat surface in a small vibration amplitude and a threshold value appears for the instability at the resonance,

$$\epsilon_c=4k_{l,m}A_c=\frac{4k_{l,m}\delta g_c}{\omega^2}=\frac{4\gamma}{\omega}. \tag{4}$$

The damping constant γ is given as

$$\gamma_b\sim\nu k_{l,m}^2 \tag{5}$$

for the bulk viscous damping and

$$\gamma_w\sim\frac{\omega l_D}{2L} \tag{6}$$

for the wall damping, where ν, $l_D=(4\nu/\omega)^{1/2}$, and L are the kinematical viscosity, the dissipation length, and the system size [7–9]. These dampings give the threshold amplitude at 3.7 K as $\delta g_{cb}\sim 4\times 10^{-3}$ m/s^2 for the bulk damping and $\delta g_{cw}\sim 0.08$ m/s^2 for the wall damping in $k_{l,m}\sim k_{0,2}$ [17]. Our sample cell is relatively small, and thus the wall damping dominated the bulk viscous damping. At 700 mK, fraction of the normal component is small [17], $\rho_n/\rho\sim 10^{-4}$, and thus δg_c caused by the damping is negligible. The observed difference in the threshold excitation between the superfluid and the normal fluid in Fig. 4 is $\Delta(\delta g_c)=0.14$ m/s^2 and on the same order of magnitude as δg_{cw} in the normal phase. The wall damping is found to be the cause of the difference in the threshold excitation between the superfluid and the

normal fluid. However, these dampings fail to explain the absolute value of δg_c. Although it would be very interesting if the superfluid had an additional damping, the excess of δg_c, which should be common to the superfluid and the normal fluid, may be due to extrinsic origin such as a misalignment of the cell, vibration direction, and so on. We have not figured out the real cause of the excess of the threshold yet. Wall velocity v estimated to be $v=A\omega\sim 2$ mm/s cannot be expected to give larger damping in the superfluid than the wall damping in the normal fluid. Peculiar features in superfluid, such as the dissipation due to the nucleation of the quantized vortices, quantum turbulence, and so on, may alter the response of the system via the larger vibration than that used in this paper.

IV. SUMMARY

We observed parametric excitation of Faraday waves in the normal fluid phase and in the superfluid phase in the low-temperature limit where the normal fluid density is negligible. The threshold amplitude for the excitation is larger in the normal fluid than in the superfluid, and the difference is explained by the wall damping in our sample cell geometry. Hysteretic behavior specific to the nonlinear waves was also observed in the superfluid phase. Additional measurements as the dispersion relation, mode identification, and various bifurcation diagrams are needed to have further insight into the Faraday instability in the superfluid.

ACKNOWLEDGMENTS

This study was supported in part by a Grant-in-Aid for Scientific Research on Priority Areas (Grant No. 17071004) from The Ministry of Education, Culture, Sports, Science and Technology of Japan and by "Ground-based Research Announcement for Space Utilization" promoted by the Japan Space Forum.

[1] M. Faraday, Philos. Trans. R. Soc. London **52**, 319 (1831).
[2] T. B. Benjamin and F. Ursell, Proc. R. Soc. London, Ser. A **225**, 505 (1954).
[3] H. W. Muller, H. Wittmer, C. Wagner, J. Albers, and K. Knorr, Phys. Rev. Lett. **78**, 2357 (1997).
[4] C. Wagner, H.-W. Müller, and K. Knorr, Phys. Rev. E **68**, 066204 (2003).
[5] P. Chen and J. Vinals, Phys. Rev. Lett. **79**, 2670 (1997).
[6] J. W. Miles, J. Fluid Mech. **146**, 285 (1984).
[7] M. C. Cross and P. C. Hohenberg, Rev. Mod. Phys. **65**, 851 (1993).
[8] S. Milner, J. Fluid Mech. **225**, 81 (1991).
[9] K. Kumar and L. S. Tucherman, J. Fluid Mech. **279**, 49 (1994).
[10] W. S. Edwards and S. Fauve, J. Fluid Mech. **278**, 123 (1994).
[11] P. Leiderer, Physica B & C **126**, 92 (1984).
[12] H. Kim, K. Seo, B. Tabbert, and G. A. Williams, Europhys. Lett. **58**, 395 (2002).
[13] R. Blaauwgeers, V. B. Eltsov, G. Eska, A. P. Finne, R. P. Haley, M. Krusius, J. J. Ruohio, L. Skrbek, and G. E. Volovik, Phys. Rev. Lett. **89**, 155301 (2002).
[14] P. Engels, C. Atherton, and M. A. Hoefer, Phys. Rev. Lett. **98**, 095301 (2007).
[15] R. Nomura, Y. Suzuki, S. Kimura, and Y. Okuda, Phys. Rev. Lett. **90**, 075301 (2003).
[16] H. Abe, Y. Saitoh, T. Ueda, F. Ogasawara, R. Nomura, Y. Okuda, and A. Ya. Parshin, J. Phys. Soc. Jpn. **75**, 023601 (2006).
[17] J. Wilks, *The Properties of Liquid and Solid Helium* (Oxford University Press, New York, 1967).